

2012

# Circulation and Water Properties and Their Relationship to the Oyster Disease MSX in Delaware Bay

Zhiren Wang

Dale B. Haidvogel

David Bushek

Susan E. Ford

Eileen E. Hofmann  
ehofmann@odu.edu

*See next page for additional authors*

Follow this and additional works at: [https://digitalcommons.odu.edu/ccpo\\_pubs](https://digitalcommons.odu.edu/ccpo_pubs)



Part of the [Marine Biology Commons](#), and the [Oceanography Commons](#)

## Repository Citation

Wang, Zhiren; Haidvogel, Dale B.; Bushek, David; Ford, Susan E.; Hofmann, Eileen E.; Powell, Eric N.; and Wilkin, John, "Circulation and Water Properties and Their Relationship to the Oyster Disease MSX in Delaware Bay" (2012). *CCPO Publications*. 70.  
[https://digitalcommons.odu.edu/ccpo\\_pubs/70](https://digitalcommons.odu.edu/ccpo_pubs/70)

## Original Publication Citation

Wang, Z., Haidvogel, D.B., Bushek, D., Ford, S.E., Hofmann, E.E., Powell, E.N., & Wilkin, J. (2012). Circulation and water properties and their relationship to the oyster disease MSX in Delaware Bay. *Journal of Marine Research*, 70(2-3), 279-308. doi: 10.1357/002224012802851931

---

**Authors**

Zhiren Wang, Dale B. Haidvogel, David Bushek, Susan E. Ford, Eileen E. Hofmann, Eric N. Powell, and John Wilkin

# Circulation and water properties and their relationship to the oyster disease MSX in Delaware Bay

by Zhiren Wang<sup>1,2</sup>, Dale B. Haidvogel<sup>1</sup>, David Bushek<sup>3</sup>, Susan E. Ford<sup>3</sup>,  
Eileen E. Hofmann<sup>4</sup>, Eric N. Powell<sup>3</sup> and John Wilkin<sup>1</sup>

## ABSTRACT

We apply a high-resolution hydro-dynamical model to investigate the role of physical factors influencing infection prevalence of *Haplosporidium nelsoni*, causative agent of MSX disease in the eastern oyster (*Crassostrea virginica*), in Delaware Bay, USA. Validation studies conducted for the years 2000 and 2010–2011 confirm that the model, based upon the Regional Ocean Modeling System, has significant skill in the recovery of observed water level, temperature, salinity, and velocity. Multi-year simulations are performed for periods representing temporal and spatial variations in *H. nelsoni* infection prevalence (1974–76, 1979–81, 1984–86, 1990–92, and 2006–09) to assess the degree to which the variations in water properties and transport are temporally and spatially correlated with infection prevalence variations. Results show statistically significant correlations between the observed prevalence of MSX and multiple physical factors including river flow and salinity (themselves highly correlated), as well as the co-occurrence of elevated temperature and salinity values. Observed occurrences of high *H. nelsoni* infection prevalence at upbay locations correspond to periods of enhanced cross-bay and upbay transport together with hospitable temperature and salinity conditions.

## 1. Introduction

Oysters (*Crassostrea virginica*) along the east coast of the United States are afflicted with, and their populations limited by, a lethal disease caused by a water-borne protozoan parasite, *Haplosporidium nelsoni* (Ford and Tripp, 1996; Powell *et al.*, 2008). The disease is called MSX disease after the acronym first given to the parasite (Multinucleated Sphere of unknown affinity). The first recorded outbreak of MSX disease was in 1957 in Delaware Bay, USA, where prevalence has continued to display significant spatial and temporal variability (Ford and Bushek, this issue). Early surveys showed that infection prevalence decreased along a decreasing salinity gradient (Andrews, 1966; Haskin and Ford, 1982). Subsequent studies demonstrated that the plasmodial stage of *H. nelsoni*, which is most common in

1. Institute of Marine and Coastal Sciences, Rutgers University, New Brunswick, New Jersey, 08901, U.S.A.

2. Corresponding author. *email: zrwang@marine.rutgers.edu*

3. Rutgers University, Institute of Marine and Coastal Sciences and The New Jersey Agricultural Experiment Station, Haskin Shellfish Research Laboratory, Port Norris, New Jersey, 08349, U.S.A.

4. Center for Coastal Physical Oceanography, Department of Ocean, Earth and Atmospheric Sciences, Old Dominion University, Norfolk, Virginia, 23508, U.S.A.

oysters, was very sensitive to low salinity and could be eliminated from oysters at salinities <10 (Ford, 1985). In contrast, the spore stage of what is presumed to be *H. nelsoni* is widely distributed throughout Delaware Bay (Barber *et al.*, 1991) and recent molecular evidence shows that the parasite can be present in upper bay and upper river sites (Ford *et al.*, 2009; Ford *et al.*, this issue).

Previous analyses of the relationship between salinity and *H. nelsoni* infection prevalence have been based on periodic salinity measurements or river flow records (Andrews, 1964, 1983; Haskin and Ford, 1982; Ford and Bushek, this issue). The availability of circulation models based upon the Regional Ocean Modeling System (ROMS) now makes it possible to investigate the relationship of water properties to MSX disease variability in Delaware Bay more quantitatively than before. Salinity and temperature are the two physical factors most likely to influence infection patterns in the bay (Ford and Haskin, 1982; Haskin and Ford, 1982). In the ROMS implementation described below, salinity in the oyster-growing area is simulated from input of six rivers (not just the Delaware), as well as precipitation, evaporation, mixing, and advection. Temperature, which is estimated from heating (including solar radiation), mixing, and advection, is the predominant correlate with seasonal infection patterns in oysters (Ford and Haskin, 1982).

With ROMS, inter-annual variations in temperature and salinity can be investigated to explore the effects of these two variables (see, e.g., Ford *et al.*, 1999 and Paraso *et al.*, 1999). In addition, ROMS permits us to investigate the role of circulation patterns in potentially moving infective stages from downbay (where prevalence is higher) into upbay regions. The method of transmission of *H. nelsoni* is unknown. To date, attempts to experimentally transmit the parasite from infected to uninfected oysters have failed and an alternate host or a vector may be involved in the life cycle (Haskin and Andrews, 1988; Ford and Tripp, 1996). A novel aspect of the circulation model is that it provides a means to test the hypothesis that *H. nelsoni* is distributed as a passive particle as opposed to a mobile host or vector with specific, nonpassive behavior.

The outline of this paper is as follows. In Section 2, the implementation and validation of the Delaware Bay model is described. Section 3 considers the inter-annual variability of, and correlations among, *H. nelsoni* infection prevalence in oysters, river flow, temperature, and salinity. Section 4 examines variability in particle transport from the lower to the upper bay. Conclusions and discussion are offered in Section 5.

## 2. The Delaware Bay model

The circulation model used in this study is the Regional Ocean Modeling System (ROMS, [www.myroms.org](http://www.myroms.org)). ROMS solves the three-dimensional hydrostatic primitive equations in terrain-following vertical coordinates using split-explicit time stepping. Computational features of importance to the simulations described below include greatly reduced pressure gradient error arising from the terrain-following coordinate, a quasi-monotone advection algorithm for the temperature and salinity fields, and alias-free coupling of the barotropic and

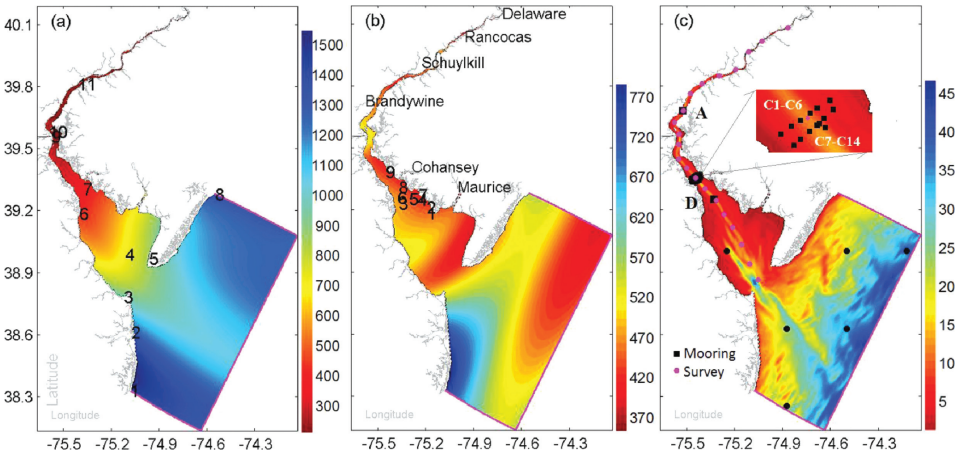


Figure 1. The Delaware Bay model implementation: (a) cross-bay spacing (m) and 11 water level stations (numbers); (b) along-bay spacing (m), 6 river inputs and 9 Versar salinity-temperature stations (numbers); and (c) bathymetry (m), locations of Delaware Bay Mooring Deployment Program (DBMDP) moorings (A, C1–C6, D), the along-bay survey locations (pink dots), and the atmospheric forcing stations (black dots). The pink boundary lines indicate the open boundaries. The depths of the water level sampling stations 1 to 11 are 10.2, 6.4, 3.2, 8.2, 5.3, 2.5, 7.4, 17.5, 4.0, 5.1, and 5.5 m, respectively. The depths at the Versar stations 1 to 9 are 6.1, 6.1, 6.5, 6.0, 4.8, 5.9, 5.4, 4.5, and 5.7 m respectively.

baroclinic modes. Shchepetkin and McWilliams (2005) describe in detail the algorithms that comprise the ROMS computational kernel. ROMS has been developed for, and successfully applied to, a wide variety of coastal marine applications, including many studies of coastal and estuarine circulation (e.g., Warner *et al.*, 2005; Liu *et al.*, 2009; Zhang *et al.*, 2009).

#### a. Model configuration

The Delaware Bay model has the following attributes. A horizontal grid of  $98 \times 386$  cells uses orthogonal curvilinear stretching to enhance horizontal resolution in the bay and tidal river compared to the adjacent coastal ocean where the domain extends to approximately the 50 m isobath (Fig. 1)<sup>5</sup>. The modeled Delaware River extends as far as Trenton, NJ, the head of the tidal regime and the location of the USGS river flow monitoring station. For the lower bay from about the Schuylkill ( $\sim 39.8^\circ\text{N}$ ) to the mouth of the bay ( $\sim 38.7^\circ\text{N}$ ), the depth of the water column ranges from approximately 3 m to 30 m, and the horizontal spacing ranges from 300 m to 1500 m. There are 20 vertical levels in a generalized topography-following coordinate weighted to give highest resolution near the sea surface. The minimum water depth is 2 m (Fig. 1c). The time step is 60 seconds and the barotropic mode is temporally integrated 25 times within each baroclinic step. Other settings include: advection via the

5. To minimize the number of “land” cells within the ROMS grid, the river cells above  $39.8^\circ\text{N}$  have been folded back onto the grid to the south. The results below will be shown in the correct, unfolded geometry.

recursive MPDATA algorithm (Smolarkiewicz and Grabowski, 1990), turbulent mixing using the Generic Length Scale (GLS) scheme (Umlauf and Burchard, 2003) with k-k1 closure parameters (Mellor and Yamada, 1982), and radiation conditions (Marchesiello *et al.*, 2001) at the open boundaries where salinity and temperature are treated using a zero-gradient condition.

### b. Simulations conducted

A total of 19 years of simulation have been conducted for two primary purposes: for model validation (years 2000 and 2010–2011; see Section 2c and the Appendix) and for exploration of inter-annual variations in observed *H. nelsoni* infection prevalence (years 1974–76, 1979–81, 1984–86, 1990–92, and 2006–09; Sections 3 and 4). In addition, various sensitivity studies have been carried out to assess operative dynamics and the influence of alternate parametric choices, including the following simulations:

- *2000A) enhanced vertical resolution*: A simulation has been conducted for the year 2000 having double the vertical resolution ( $N = 40$ ). This modification makes negligible difference to model skill or to the results reported below.
- *2000B) alternative values for the ROMS water type*: “water type” regulates the vertical penetration of solar shortwave radiation. After sensitivity studies employing alternative values for the water type, a water type of 7 was identified as the best choice. See Section 2c.
- *2008A) no wind*: To investigate the role of wind forcing, a simulation for 2008 has been carried out with atmospheric wind stress removed.
- *2008B, 2011B) increased bottom stress*: To examine the role of bottom stress in regulating the amplitude of the tidal currents, we have re-run years 2008 and 2011 with a bottom resistance coefficient increased by 50%.

Further discussion of these sensitivity studies is offered below.

### c. Forcing data

ROMS is forced by the following inputs: 6-hourly atmospheric fluxes (for the 1974–76 simulation) from the ERA-40 data of European Centre for Medium-Range Weather Forecasting (ECMWF, <http://data-portal.ecmwf.int>) and 3-hourly atmospheric fluxes (for all the other simulations) from the North American Regional Reanalysis (NARR; Mesinger *et al.*, 2006) input at six locations (Fig. 1c). Daily river transport from US Geological Survey (USGS, <http://waterdata.usgs.gov>) is introduced at six locations (Fig. 1b). Annually averaged river transport from the six rivers varies between 283 to 880 m<sup>3</sup>/s with the majority (roughly 75%; Table 1) being contributed by the Delaware River and secondarily by the Schuylkill River (~18%). Tidal elevation and currents at the domain perimeter with seven tidal constituents ( $M_2$ ,  $N_2$ ,  $S_2$ ,  $K_1$ ,  $O_1$ ,  $M_4$ , and  $M_6$ ) are provided from the North Atlantic regional harmonic tidal simulation (Mukai *et al.*, 2002). No subtidal water level information is provided at the open boundaries.

Table 1. Annual mean freshwater discharge rate into Delaware Bay from the six rivers included in the model (Fig. 1b). The mean values shown are for the entire period from 1974–2011.

year	Delaware		Schuylkill		Brandywine		Maurice		Rancocas		Cohansey		Total
	m <sup>3</sup> /s	%	m <sup>3</sup> /s	%	m <sup>3</sup> /s	%	m <sup>3</sup> /s	%	m <sup>3</sup> /s	%	m <sup>3</sup> /s	%	m <sup>3</sup> /s
1974	385	78.5	79.7	16.3	12.3	2.5	4.1	0.8	5.0	1.0	4.1	0.8	<b>490</b>
1975	449	73.4	123	20.2	20.3	3.3	6.5	1.1	6.2	1.0	6.5	1.1	<b>612</b>
1976	363	77.7	79.7	17.0	12.4	2.7	4.0	0.9	4.0	0.9	4.0	0.9	<b>467</b>
1979	446	73.9	109	18.1	25.4	4.2	7.6	1.3	7.8	1.3	7.6	1.3	<b>604</b>
1980	229	75.3	51.2	16.9	11.5	3.8	4.2	1.4	3.8	1.2	4.2	1.4	<b>304</b>
1981	225	79.3	43.0	15.2	6.7	2.4	2.9	1.0	3.1	1.1	2.9	1.0	<b>283</b>
1984	386	71.6	113	21.0	20.8	3.9	6.3	1.2	6.4	1.2	6.3	1.2	<b>539</b>
1985	249	77.8	53.2	16.6	8.4	2.6	3.4	1.1	2.7	0.8	3.4	1.1	<b>320</b>
1986	354	79.3	70.4	15.8	10.6	2.4	3.7	0.8	3.9	0.9	3.7	0.8	<b>446</b>
1990	387	77.3	86.4	17.3	12.5	2.5	4.7	0.9	5.3	1.1	4.7	0.9	<b>500</b>
1991	243	74.5	60.2	18.5	10.3	3.2	4.1	1.3	4.5	1.4	4.1	1.3	<b>326</b>
1992	266	76.7	61.6	17.8	9.1	2.6	3.1	0.9	4.0	1.1	3.1	0.9	<b>346</b>
2000	339	76	80.9	18.1	14.7	3.3	3.9	0.9	4.1	0.9	3.9	0.9	<b>447</b>
2006	482	77.0	114	18.3	14.8	2.4	4.8	0.8	5.1	0.8	4.8	0.8	<b>625</b>
2007	367	76.3	85.4	17.8	14.5	3.0	4.8	1.0	4.6	1.0	4.8	1.0	<b>481</b>
2008	435	80.2	85.5	15.8	11.6	2.1	3.3	0.6	3.6	0.7	3.3	0.6	<b>543</b>
2009	370	74.7	96.1	19.4	14.7	3.0	4.8	1.0	4.9	1.0	4.8	1.0	<b>495</b>
2010	364	75.4	85.1	17.6	15.9	3.3	6.1	1.3	5.4	1.1	6.1	1.3	<b>483</b>
2011	691	78.5	146	16.6	21.6	2.5	7.7	0.9	5.9	0.7	7.7	0.9	<b>880</b>
Mean	<b>362</b>	<b>75.7</b>	<b>87.8</b>	<b>18.4</b>	<b>14.4</b>	<b>3</b>	<b>4.6</b>	<b>1</b>	<b>4.8</b>	<b>1</b>	<b>4.6</b>	<b>1</b>	<b>478</b>

A summer-time discrepancy in heating rate was traced, in part, to the incoming solar short-wave radiation. The solar shortwave radiation (hereafter, SSWR) from the North American Regional Reanalysis was discovered to be systematically higher than concurrent values given by the Delaware Environmental Observation System (DEOS). Comparing 5-min interval DEOS SSWR and 3-hr interval NARR SSWR within Delaware Bay for the period 2005–2009 when both DEOS and NARR SSWR are available (Fig. 2) we find ratios of DEOS to NARR SSWR of 77.4%, 77.1%, 76.7%, 76.2%, and 76.8% respectively for winter, spring, summer, fall, and the whole year. The systematic difference is nearly independent of season, so we make a simple correction in the simulations reported below by reducing NARR SSWR by 20%.

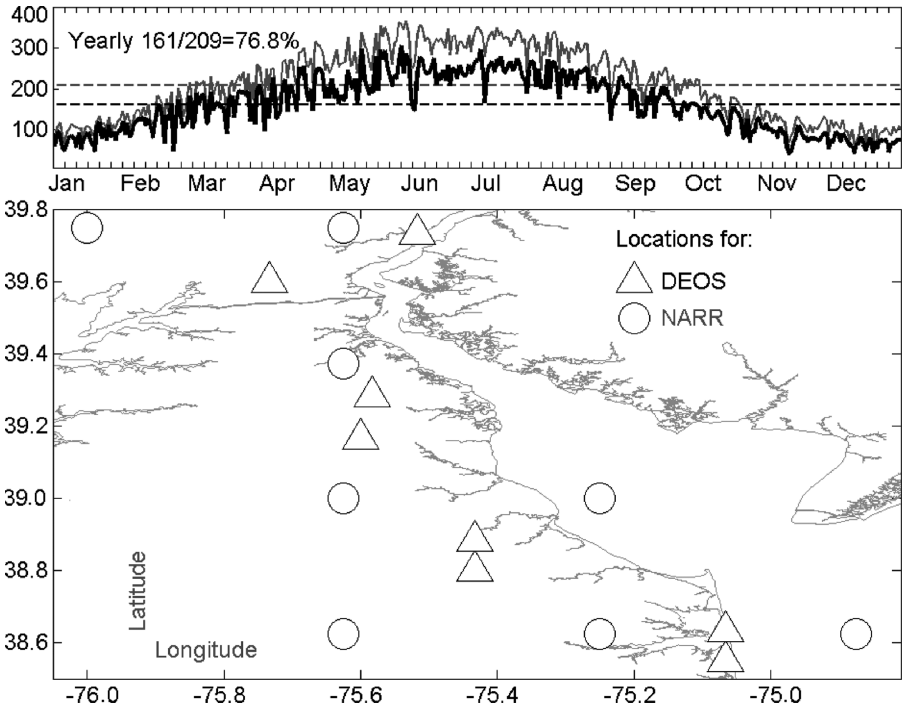


Figure 2. NARR and DEOS solar short wave radiation ( $Wm^{-2}$ ): (lower panel) locations of the DEOS and NARR observing stations; (upper panel) mean annual variation in NARR (grey) and DEOS (black) SSWR computed as an average over years 2005 to 2009. DEOS: Delaware Environmental Observation System, NARR: North American Regional Reanalysis.

The temperature of the shallow water column is sensitive to the net heat flux, but also to the depth scale assumed for solar radiation absorption. In ROMS, this absorption profile is represented as two exponential functions following Paulson and Simpson (1977) with parameters determined by an assumed “water type” that defines the fraction of incident solar shortwave radiation flux penetrating the water column to a specified depth ( $z < 0$ ):  $Ae^{z/B} + (1 - A)e^{z/C}$ . Here, A is the relative amount of red light incident on the sea surface, and B and C are attenuation lengths (m) for the red and blue-green bands, respectively. After correction of the NARR SSWR data, sensitivity studies (2000B) showed ROMS water type 7 – corresponding to  $A = 0.5$ ,  $B = 0.2$  m, and  $C = 0.2$  m – to produce the most accurate hindcasts<sup>6</sup>. Water type 7 is consistent with the often turbid conditions over much of Delaware Bay. (See also Cahill *et al.*, 2008.)

6. Water type 7 confines SSWR absorption to a very shallow surface layer, thereby influencing the surface heat and moisture budgets. When compared to water types 5 and 6, the use of water type 7 reduces summertime water column temperatures by approximately 0.5 degrees and increases surface salinity by 0.1–0.3.

#### d. Model validation

We choose observations of water level, temperature and salinity in the year 2000, and salinity, temperature and currents observed in 2010–2011 as the datasets for model validation. These time periods were chosen because relatively good observations of water properties and circulation are available.

The year-2000 water level observations are obtained from the National Water Level Program (NWLP) and the National Water Level Observation Network (NWLON) at <http://tidesandcurrents.noaa.gov>. There are eleven stations (Fig. 1a) in Delaware Bay where the observed water levels are available. The recording interval is one hour.

Observed water temperature and salinity at one-meter from the bottom at the nine oyster beds (Fig. 1b) in the year 2000 are provided by the Pre-Construction Oyster and Water Quality Monitoring Study for the Main Channel Deepening Project [prepared by Versar, Inc., <http://www.versar.com>]. Their recording interval is 15 minutes for the period 13 May–12 November 2000 and from 8 March–12 April 2001. The temperature signals are dominated by the seasonal cycle, while the salinity time series have both tidal and lower-frequency components (not shown).

More recently, an array of instrumented moorings combined with shipboard surveys have been deployed seasonally by the Delaware Bay Mooring Deployment Project (DBMDP; Chant, personal communication, 2012). As shown in Figure 1c, the DBMDP included 16 moorings (A, C1–C14, and D) where salinity, temperature, and currents are observed at multiple depths and with high temporal resolution. In addition, five along-bay surveys (12–13 September 2010, 13–14 December 2010, 21–22 March 2011, 3–4 June 2011, and 16–17 September 2011) were conducted to observe the spatial structure of the salinity and temperature fields from about 38.9°N to 40.1°N (Fig. 1c).

The results of the model validation study may be summarized as follows. A more complete description of the findings is contained in the Appendix.

*i. Water level (2000).* ROMS does a highly skillful job in simulating water levels. For a period of 204 days (11 June to 31 December, 2000) with 4896 hourly samples, skill scores exceed 95% at all eleven water level stations. Tidal excursion, as measured by normalized standard deviation of the simulated water level, is well predicted in the lower bay, but higher than observed by approximately 30% in the upper bay. We discuss a possible cause for this below.

*ii. Water temperature (2000).* Temperature time series at the nine Versar sampling sites are dominated by the seasonal cycle. ROMS reproduces temperatures at the Versar sites with great accuracy. Skill scores exceed 99% at all locations, and temperature variability is also highly accurate. Bias in the temperature time series is within 0.4°C, and typically much less. The high skill reflects the fact that the temperature is dominated by the seasonal cycle. The correlation coefficient between the observed and simulated temperature is above 0.99. It is reduced to 0.6~0.95 (station-dependent) with the annual cycle removed. For the shallow coastal water column, different incoming solar radiation levels make a significant difference. The original NARR SSWR was initially observed to make the bay too warm by about 0.6 to 1.4°C (not shown).

*iii. Salinity (2000).* Salinity time series at the nine Versar stations show strong contributions at both tidal frequencies and at longer periods associated with variations in freshwater inputs. Salinity values decrease towards the upper bay and are closely tied to river inputs, as shown more quantitatively below. The correlation coefficients between simulated and observed salinities are higher than 0.8 at all but one station; the outlier is at station 1, the most downbay location. Skill scores vary between 88% and 93%, except at station 1 (78%). The standard deviations of simulated salinity are close to those observed. Finally, the systematic bias in salinity exceeds 1 at only one station; it is 1.1 at station 9, the most upbay Versar station.

*iv. Along-bay currents (2010–2011).* For purposes of analysis, the simulated and observed vector currents have been decomposed into their along- and across-bay components, as determined by principal component analysis of the depth-integrated currents at each mooring site. Statistical comparison of the observed and simulated depth-integrated, along-bay currents at nine locations (moorings A, C1, 2, 6, 8, 9, 11, 14 and D – see Appendix) shows high correlation ( $>0.85$ ), high skill ( $>0.88\%$ ) and low bias ( $<0.10$  m/s). However, current variability is systematically high by between 10 and 40%, except at the upbay mooring A. This is consistent with the over-estimation of water level variability noted above. If the bottom resistance coefficient is increased by 50% (experiment 2011B), the comparison between observed and simulated current variability is improved in the lower bay, but degraded in the upper (not shown). A properly chosen spatially dependent bottom stress coefficient would be required to simultaneously improve currents everywhere in the bay.

*v. Along-bay structure of the temperature and salinity fields (2010–2011).* In addition to proper reproduction of temporal variability at points within the bay where time series are available, it is important to examine the fidelity of the spatial structure of the simulated fields. One such metric is the along-bay distribution of temperature and salinity, and their vertical differences (i.e., the stratification). The data from the 5 along-bay DBMDP transects in 2010–2011 allow us to examine these spatial issues. We are particularly interested to determine if ROMS shows skill in the recovery of the along-bay location and vertical (top-to-bottom) salinity difference in the salt wedge. This comparison shows that ROMS again displays high correlation and skill, and low bias in the recovery of along-bay salt stratification (Appendix, Fig. A2).

*vi. Interpretation.* The foregoing validation is reassuring. But are these results “good enough?” The answer to this question is dependent on the purposes to which the simulated tracer and velocity fields will be applied. In this issue, the simulated fields from the Delaware Bay model are used for two types of studies. First, we utilize the simulations to inquire into the relationships between water properties and the observed prevalence of MSX (this contribution) and between those properties and observed food resources (Powell *et al.*, this issue). Second, model outputs (temperature, salinity, and currents) are used as inputs to the oyster larval behavior studies of Narváez *et al.* (this issue, a,b). It is perhaps the latter larval individual-based modeling (IBM) studies that place the greatest burden on the fidelity of the simulated temperature and salinity fields. In the IBM, larval success depends sensitively

on the ambient temperature and salinity values which the larvae encounter. Successful reproduction of larval growth and behavior will depend on many factors, but environmental fields accurate to within 1°C in temperature and 1 in salinity would be a reasonable tolerance to require given the details of the IBM (Narvaez *et al.*, this issue, a). The validation studies carried out here show the ROMS simulations to satisfy this requirement. We have already noted above that tidal current amplitudes are dependent on the value of the bottom stress coefficient. This is one area where an alternative formulation (e.g., a spatially dependent stress coefficient) could offer an improvement. Nonetheless, as will be seen from sensitivity study 2008B (Section 4), variations in the bottom stress do not materially alter the primary transport pathways in the model.

### 3. Inter-annual changes in *Haplosporidium nelsoni* infection prevalence, river flow, temperature and salinity

*Haplosporidium nelsoni* infection prevalence (hereafter, MSXP) has been assayed one to two times per year on 5 sites in Delaware Bay (Arnolds, Cohansey, New Beds-Bennies, Egg Island and Leased Grounds) since 1958, shortly after the initial outbreak. Between 1958 and 2010, all beds were assayed in fall (October/November). From 1958 through 1991 the beds were also assayed in spring (May). These months represent annual infection peaks (Ford and Haskin, 1982). Figure 3 shows a time series of MSXP at five locations within the bay, accompanied by a similar time series for Delaware River discharge at Trenton, New Jersey. General patterns of MSXP include a systematic downbay increase, where higher salinity favors the parasite, with lower values at the upbay locations. Freshwater inflow at Trenton is larger in winter/spring by a factor of about two over summer/fall. Lastly, note the reduced downbay prevalence of MSXP associated with the development of increased resistance after 1987 (Ford and Bushek, this issue).

Prior studies (Andrews, 1964; Haskin and Ford, 1982) suggest that the upbay prevalence of *H. nelsoni* is highly correlated with fluctuations in salinity, and therefore with freshwater inflow. This relationship is strongest in the spring, when typically high freshwater inflow depresses or eliminates *H. nelsoni* infections from oysters in the upper bay (Haskin and Ford, 1982). When the spring runoff does not occur, infections persist, sometimes causing catastrophic mortality (Ford and Bushek, this issue).

Rather than a single determining factor, we hypothesize that MSXP at upbay locations is related to the co-occurrence of three factors. These are: (1) the availability of infective elements (mostly likely from a downbay source), (2) a transport mechanism from lower- to upper-bay locations, and (3) environmental conditions (i.e., temperature and salinity) conducive to *H. nelsoni* survival and ability to proliferate in oysters. If any one of these factors is lacking, then upbay MSXP will be reduced. For instance, if a source of infective elements is not present, neither favorable transport nor favorable environmental conditions will lead to significant MSXP in upbay oysters.

To investigate these hypothesized relationships, we have selected five multi-year periods for study. The periods selected for simulation represent temporal and spatial variations of *H.*

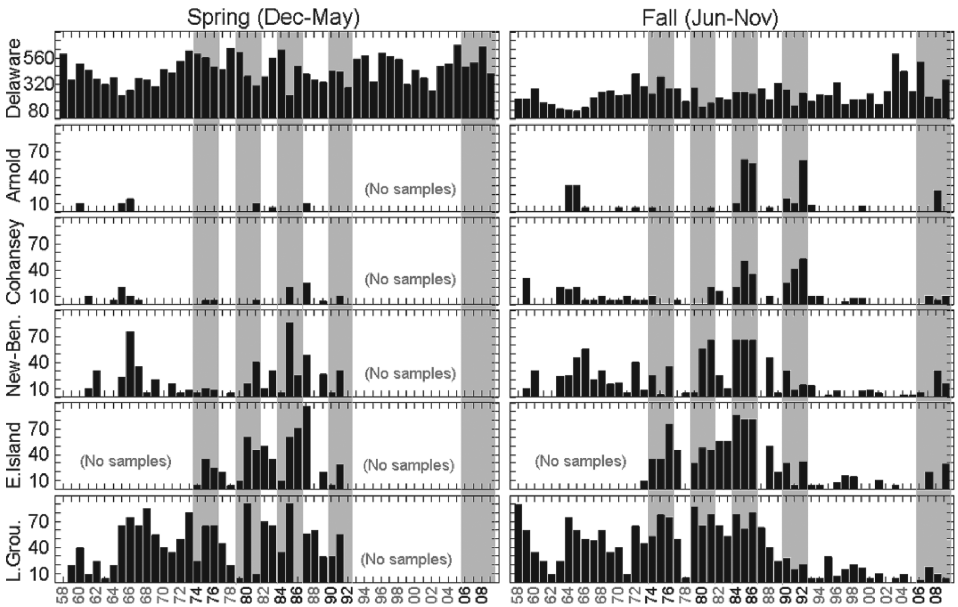


Figure 3. Time series of spring (Dec–May, column 1) and fall (Jun–Nov, column 2) Delaware River flow ( $\text{m}^3/\text{s}$ , row 1) and *Haplosporidium nelsoni* prevalence (MSXP, %) at Arnolds, Cohansey, New Beds-Bennies, Egg Island, and Leased Grounds (rows 2–6). The highlighted periods 1974–76, 1979–81, 1984–86, 1990–92, and 2006–09 are the five scenarios used for our comparison. MSXP is defined as  $100 \times \text{number of infected oysters}/\text{number of oysters sampled}$ .

*nelsoni* infections in oysters at these locations in relation to Delaware River flow measured at Trenton, New Jersey (Table 2). The five periods, and their respective overall properties, are: 1974–76 (average/above average river flow, low upbay MSXP), 1979–81 (average river flow, low upbay MSXP), 1984–86 (average river flow, high upbay MSXP [especially 1985–86]), 1990–92 (average river flow, high upbay MSXP [especially 1992]), and 2006–09 (average/above average river flow, elevated upbay MSXP in 2008). The particle transport is simulated for period 2007–2009 and the effects on particle transport from winds and enhanced bottom drag are further explored for 2008 when the MSXP is elevated upbay.

Mean wind vectors in spring (May–June, not shown) vary rather little across the 16 years studied here. They are directed cross-bay from southwest to northeast at speeds of  $\sim 1$ –2 m/sec in all but one year (1992, in which mean spring winds are weak and directed to the northwest). The strongest cross-bay spring winds in our five periods occur in 1976 and 2008. Mean winds in the fall (September–October) are weaker than in spring and more variable in direction, though with a westerly component in all years but two (1984, 2009). As will be shown below, particle transport in these simulations is primarily due to the combined effects of riverine and tidal forcing, with wind forcing of secondary importance.

By contrasting these five periods, we hope to address several questions. These include the following. How much variability in MSXP can be accounted for purely on the basis of

Table 2. Rationale for selection of model simulation periods based on *Haplosporidium nelsoni* prevalence (MSXP) in oysters in Delaware Bay compared to Delaware River flow measured at Trenton, New Jersey. Prevalence was assessed using tissue-section histology for the first four periods and using both histology and polymerase chain reaction (PCR) for the last.

Period	1974–1976	1979–1981	1984–1986	1990–1992	2006–2009
Prevalence	elevated in lower bay, reduced in upper bay	(Same as in 1974–1976)	very high with extreme mortality	very high on uppermost beds in 1991–1992, low elsewhere	elevated on uppermost beds in fall2008 -spring2009
River flow	average or above average	below average 1980–1981	drought Sep1984 -Aug1985	below average fall1991 -spring1992	average or above average

salinity variations, temperature, or both? Is there any evidence for the hypothesized role of upbay passive transport? And finally, is there any evidence for limitation due to the absence of a downbay source?

#### *a. Variations in physical properties*

Simulations of the water properties and circulation in Delaware Bay for the five multi-year periods (1974–76, 1979–81, 1984–86, 1990–92, and 2006–09) have been conducted. Subsequent statistical analysis was then employed to explore the quantitative relationships among the variations of prevalence and physical conditions in the bay.

In addition to investigating the individual roles of salinity and temperature, we explore a combined index, the “salty-warm water area” (SWA), which we define as the area of the bay whose bottom salinity is higher than 17.5 and whose bottom temperature is higher than 12.5°C. These values represent conservative estimates of the lower thresholds for *H. nelsoni* proliferation in oysters (Ford and Haskin, 1982; Haskin and Ford, 1982). It will be noted below that salinity and temperature are negatively correlated; therefore, the co-occurrence of warm and salty conditions, while potentially beneficial to the proliferation of MSX, is expected to be rare but did occur in 1984–1986.

Figure 4 displays time series for our five multi-year periods (16 years in total) of the following physical properties: the total freshwater inflow of the six river inputs, the bottom-average salinity at several locations within the bay (Arnolds, Cohansey, Egg Island, as shown in Fig. 5), bay-average bottom temperature<sup>7</sup>, and salty-warm water area. Also shown are anomalies for each of these quantities. Anomalies for temperature and SWA are obtained by removal of a 16-year mean seasonal cycle; anomalies for salinity and river flow are formed by removal of a 16-year mean value (i.e., by removal of a constant from the time series at a given location).

Considerable inter-annual variation in the physical environment is evident. A brief summary of these variations is as follows:

- **1974–76:** River input is the second highest among the five multi-year periods (47 m<sup>3</sup>/s higher than the long-term mean of 478 m<sup>3</sup>/s). Salinity is slightly below the 16-year average, with the most negative anomalies at Arnolds (−0.6) and Cohansey (−0.5), the two uppermost sites sampled. The three-year-mean temperature is close to the longer-term mean. SWA is near the long-term average.
- **1979–81:** River flow is low (81 m<sup>3</sup>/s below the long-term mean) for an extended period from May 1980 to January 1981 and from August to October of 1981. Mean conditions in 1979–81 are both the saltiest (Arnolds, +1.6; Cohansey, +1.3; Egg Island, +1.1) and coolest (−0.8°C) of our five time windows. SWA is the smallest of any of the multi-year periods.

7. Bottom temperature is highly correlated (0.98) with concurrent air temperature, and varies little across the bay, except in the deep channel where it is somewhat warmer (0.5°C) in winter and colder (2–4°C) in summer.

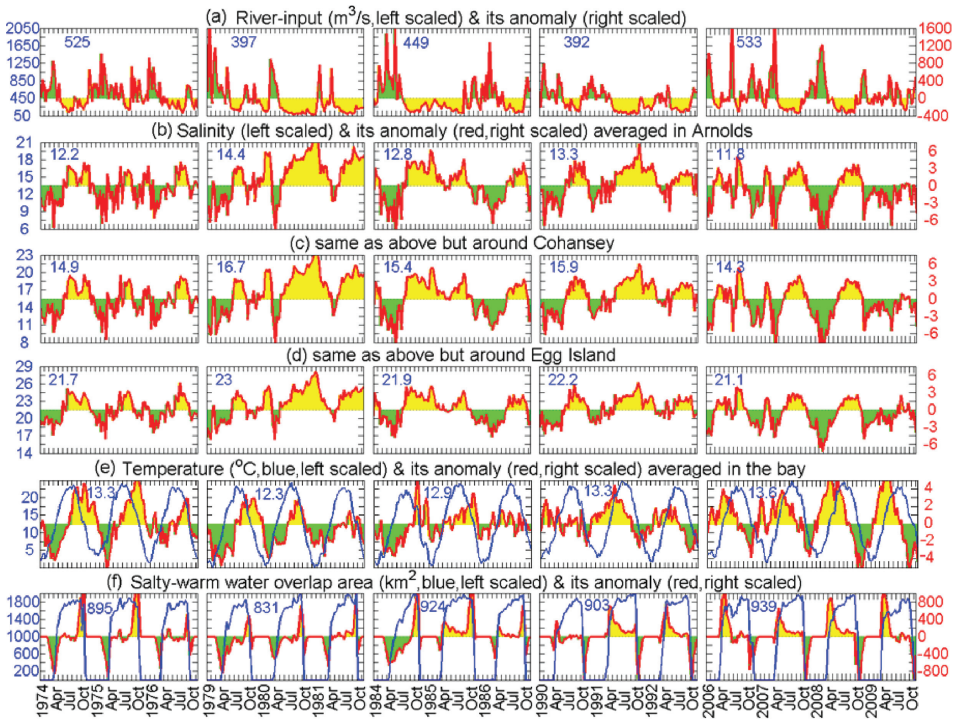


Figure 4. Ten-day-averaged time series (left scales) and their anomalies (right scales) for: a) the total river discharge ( $\text{m}^3/\text{s}$ ); b,c,d) the simulated bottom salinity averaged within beds; e) bottom temperature ( $^{\circ}\text{C}$ ) averaged within the bay; and f) the salty-warm water area (SWA,  $\text{km}^2$ ). In (f), the SWA (blue lines) refers to the area of the bay whose bottom salinity/temperature is higher than  $17.5/12.5^{\circ}\text{C}$ . The anomalies are relative to the means within the sixteen years (1974–76, 1979–81, 1984–86, 1990–92, and 2006–09) with seasonality deducted only for temperature and SWA. Within each frame, during yellow/green-shaded periods the anomaly is positive/negative continuously for over twenty days. The blue number in each frame indicates the total mean within each scenario.

- 1984–86:** River input in this three-year period is near the 16-year mean and both salinity and temperature are “spot on” the 16-year mean values. SWA is high (+23  $\text{km}^2$  larger than the long-term mean of 901  $\text{km}^2$ ). Although the three-year means are near the long-term average, there are identifiable periods of above- and below-average salinities. Of particular significance is an extended period of above-average upbay salinity from approximately July 1984 to September 1985 corresponding to a period of reduced river inflow. An eight-month period, the longest of any of the multi-year periods, of both warmer and saltier conditions starting from April till November 1985 was not broken by a significantly cold or fresh phase as they were in the other four multi-year periods, making SWA persistently higher than average during this period.

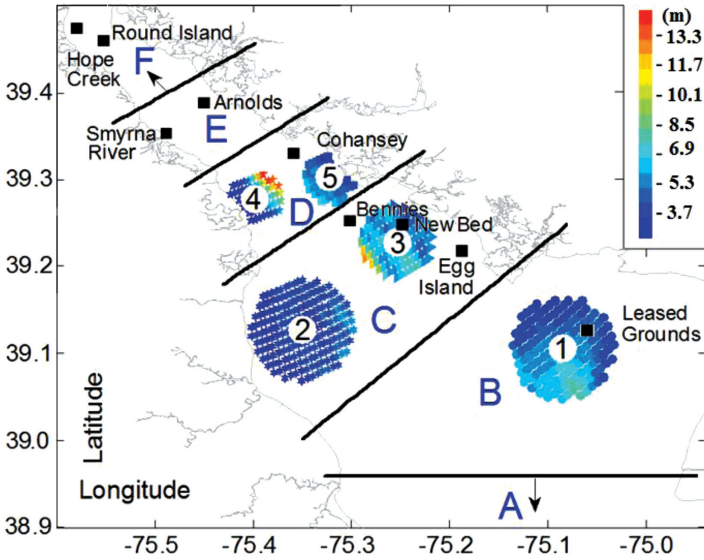


Figure 5. Locations of the major oyster collection sites (black squares), released floats (colored shapes), and transport/retention regions (separated by straight lines). There are 141, 194, 106, 59, and 50 releasing grid points within the five circular areas (1–5, respectively). On each grid point ten floats are released (five at bottom, five near bottom, at three-hour intervals) on each of the release days: 1, 15 and 29 May, 12 and 26 June, 15 and 29 August, 12 and 26 September, and 10 October. The color bar indicates the releasing depth (m) averaged between the two releasing layers. Six regions (A, B, C, D, E, and F) are used to locate floats.

- **1990–92:** On average, this three-year period is a bit warmer (+0.2°C) and saltier (Arnolds, +0.5; Cohansey, +0.5; Egg Island, +0.3). The latter is associated with drier conditions (3-year mean river flow 86 m<sup>3</sup>/s below the long-term mean). SWA is near normal.
- **2006–09** is the warmest period (+0.5°C), and is accompanied by the largest river flow (+55 m<sup>3</sup>/s). Given the increased river inputs, salinities are lower than in any other period (Arnolds, -1.0; Cohansey, -1.1; Egg Island, -0.8). The averaged SWA is enhanced above the long-term mean (+38 km<sup>2</sup>); however, no positive SWA anomaly phase lasts longer than eight months as in 1985–86.

*b. Correlation analysis*

To examine the quantitative relationships between MSXP and accompanying environmental conditions, we have performed a systematic correlation analysis, seeking significant correlations between factors including: fall (June–November), spring (December–May) and yearly MSXP; monthly, seasonal (DJF, MAM, JJA, and SON), and yearly river discharge and simulated salinity and temperature. Correlations of total river flow integrated from the

six rivers whose locations are shown in Figure 1b with MSXP are based upon seasonal observations in 1958–2009, with the sample size being 52. The simulated salinity, temperature and SWA in 1974–76, 1979–81, 1984–86, 1990–92, and 2006–09 are used to correlate with each other and with river discharge and MSXP with the sample size being 12 in spring and 16 in fall. (Spring samples of MSXP are not available for the 2006–2009 period.) The data availability of MSXP and the rationale for selection of model simulation periods (Table 2) together dictate our data sample sizes.

Correlations among these variables have been computed for five locations within the bay: Arnolds, Cohansey, New Beds-Bennies, Egg Island, and the Leased Grounds as shown in Figure 5. Values for salinity and temperature have been obtained from the simulations by averaging in a 2-by-2 km area centered on these locations. The seasonal cycles have been removed from the bottom temperature and SWA since they are dominated by the seasonal cycle.

We note that resistance of oysters to MSX develops after the early 1990s (Fig. 3; Ford *et al.*, this issue). The correlations described below have been obtained using all years for which MSXP data are available; i.e., we have included MSXP values from the contemporary period during which disease resistance appeared. The primary conclusions of the correlation analysis are unchanged if the contemporary period is omitted.

*i. Physical properties.* Correlations have been obtained between the river flow (the sum of the six rivers included here) and the 16-year simulated bottom salinity and bottom temperature averaged in a two-by-two kilometer square around each of the above-mentioned five areas. As expected, river flow and simulated salinity are highly negatively correlated at all locations (mean correlation at the five beds  $-0.80$ ). There is also a statistically significant positive correlation between river flow and temperature in both winter/spring (five-bed mean  $0.62$ ) and summer/fall ( $0.49$ ), presumably a reflection of a positive relationship between temperature and winter/spring snowmelt and summer/fall convection and precipitation. The negative river flow/salinity and positive river flow/temperature correlations dictate a negative temperature/salinity correlation (five-bed mean  $-0.64$ ).

*ii. MSXP.* Several correlations between the physical environment and MSXP are statistically significant at either the 90% or 95% confidence level (Table 3). We anticipate that *H. nelsoni* proliferation will be discouraged by unfavorable concurrent environmental conditions. In particular, lower values of salinity, or the associated enhanced river flow, should be closely related to observed MSXP. From Table 3, we see that this assumption is confirmed. Statistically significant negative correlations between spring (December–May) MSXP and December–May river flow hold at three of the five beds (Cohansey, New-Bennies, Leased Grounds). The correlation between MSXP and simulated salinity is also significant at Arnolds.

New *H. nelsoni* infections are acquired, and residual infections begin to proliferate, in late spring. Therefore river flow in the spring must also correlate with MSXP measured in the fall of that year. Significant, though small, negative correlations with river flow in the preceding spring are shown to hold for MSXP observed in the fall at two beds (Arnold

Table 3. Correlation coefficients (Corr.), effective degrees of freedom (EDF), and confidence of the correlations between *Haplosporidium nelsoni* infection prevalence (MSXP) and total river flow input from the six rivers whose locations are shown in Figure 1b, and with salinity and salty-warm water area at the Arnolds, Cohansey, New-Bennies, Egg Island, and Leased Ground locations shown in Figure 5. The bold black and grey-shaded numbers indicate the correlations with rejecting probability 5% or less and 5~10%, respectively. The correlation coefficients have been obtained using the Matlab functions corr and corrcoef. The effective degrees of freedom (Emery and Thomson, 2004) are evaluated using the general formula given by Chelton (1983).

Locations	Spring river flow / Spring MSXP		Spring salinity / Spring MSXP		Spring river flow / Fall MSXP		Directly preceding fall SWA / Spring MSXP	
	Corr.	EDF	Corr.	EDF	Corr.	EDF	Corr.	EDF
Arnolds	-0.31	15.8	<b>0.71</b>	7.0	-0.29	32.1	0.01	
Cohansey	-0.46	14.0	0.48	8.3	<b>-0.39</b>	31.5	<b>0.91</b>	4.0
New Bennies	-0.52	10.3	0.59	5.9	-0.29	29.5	<b>0.92</b>	4.2
Egg Island	-0.48	7.3	0.46	5.3	-0.16		0.55	5.2
L. Grounds	-0.27	36.0	0.38	9.0	-0.10		0.52	4.1

and New-Bennies; Table 3). In contrast to the highly significant correlation of river flow (and therefore salinity), especially at the upbay locations, the correlation analysis indicates that temperature by itself does not appear to play a significant role in MSXP variation. The apparent explanation for this result is that temperature also negatively influences salinity (64% negatively correlated). Elevated temperatures, by themselves, are generally conducive to MSXP for the prevailing spring and summer temperature ranges in Delaware Bay (Ford and Haskin, 1982). However, higher water temperatures are also associated with higher riverine input (68% positively correlated) and reduced salinities, which are detrimental to proliferation. The two effects counteract, with the result that temperature is not, by itself, well correlated with MSXP.

Finally, the co-occurrence of warmer temperatures with more saline conditions is relatively rare. However, when these conditions arise, as in 1984–86, the environment is especially conducive to elevated MSXP. Indeed, from Table 3 we see that SWA is highly correlated with MSXP at both Cohansey (0.91) and New-Bennies (0.92) and of somewhat less significance at Egg Island and Leased Grounds. The elevated correlation with SWA at mid-bay locations is due to the fact that variations in salinity about the value 17.5 are greatest at mid-bay. The SWA metric has essentially zero explanatory power at upper-bay sites such as Arnolds because salinity values rarely, if ever, exceed 17.5 at these locations. (That is, the area covered by the salty and warm water never reaches the most upbay sites.) Likewise, salinity values typically exceed 17.5 at the most downbay locations. There, the correlations with the SWA metric are reduced because the water is always salty enough for proliferation.

### c. Relationship to enhanced upbay MSXP

We have a particular interest in the occurrences of enhanced MSXP at upbay sites such as Arnolds, and the mechanisms responsible for them. Among the fall surveys covered in our 16 years of simulations, there are three occasions in which noticeable year-to-year increases in MSXP occur at Arnolds. These years are 1985, 1992 and 2008 (Fig. 3).

The significant correlations between MSXP and local environmental conditions detailed above suggest that these three periods of elevated MSXP might correspond to years in which conditions were particularly suitable to *H. nelsoni* proliferation. And indeed, the time series shown in Figure 4 confirm that this was indeed the case for the fall 1985 and fall 1992 surveys. In both instances, the surveys were preceded by a lengthy period (>1 year) of reduced river flow and correspondingly elevated salinity. While other causative agents cannot be ruled out, it seems likely that conducive local conditions were responsible for the upbay outbreaks in 1985 and 1992. (Note also that downbay sources of *H. nelsoni*, as inferred from MSXP, were abundant in 1985. Lower downbay MSXP in 1992 is related to the development of resistance to MSX disease after 1987, although this does not necessarily mean a lack of infective elements, as discussed below.)

Unfortunately, the explanation of favorable environmental conditions does not so easily fit the observations from the fall 2008 survey. While salinity is somewhat elevated in fall 2008, the preceding spring is anomalously wet and fresh. As in 1992, the low downbay MSXP (Fig. 3) is a reflection of resistance not absence of *H. nelsoni*. In fact, the use of a very sensitive molecular detection assay, polymerase chain reaction (PCR), showed a spike in the presence of *H. nelsoni* in the environment in fall 2008, even though MSXP was only marginally elevated (Ford *et al.*, this issue). Different, or perhaps additional, mechanisms besides beneficial environmental conditions must have been at work in 2008.

## 4. Particle transport between the lower and upper bay

Above, we have hypothesized that factors in addition to temperature and salinity – such as the availability of an effective lower-bay source region, and an efficient upbay transport mechanism – might also be related to the presence or absence of *H. nelsoni* in upper-bay regions. Conversely, there could be an effective source and sufficient upbay transport, but a lack of adequate environmental conditions or other factors necessary to produce and/or maintain *H. nelsoni* infections (e.g., another host; Haskin and Andrews, 1988).

During a 3-year (2007–2009) study of potential disease refuges in the upper bay, the presence of *H. nelsoni* was monitored using both histological and molecular methods (Ford *et al.*, this issue). The increased sensitivity of the PCR assay permitted detection of a particularly striking example of upbay incursion of *H. nelsoni* that occurred in summer/fall 2008.

Although the average upbay conditions in the overall period 2006–2009 were somewhat fresher and warmer than their respective longer-term means, the summer/fall months (June through November) of 2008 were relatively salty (Fig. 4). These conditions would be hospitable to *H. nelsoni* if a source to the upper bay were available.

Here, we explore the simplest possibility: that the pulse of *H. nelsoni* infective elements apparently introduced into the upper bay in the summer of 2008 is related to enhanced upbay transport of passive particles<sup>8</sup>. To do so, we simulate the trajectories of passive particles<sup>9</sup> released near and at the sea bed at the horizontal locations shown in Figure 5. The particles are released at five locations within the bay (labeled 1 through 5 in Fig. 5), and during each of three years (2007–2009) on ten different days (1, 15 and 29 May; 12 and 26 June; 15 and 29 August; 12 and 26 September; and 10 October). On each of these days the particles are released five times at three-hour intervals to cover approximately one  $M_2$  period. The number of particles released in each location 1–5 is proportional to the number of circles shown in Figure 5.

The passive particles are tracked from their release time to 31 October of the year unless they leave the water of the bay. The result is a set of time series of particle locations for passively redistributed water parcels. These time series may then be subjected to analysis to determine the likelihood that particles released at a given location will be transported by either advection or mixing into other regions. The sub-regions for which this analysis is performed are labeled A through F in Figure 5. We are particularly interested in the pathways by which, and effectiveness with which, particles reach the upbay regions labeled E and F.

#### *a. General patterns of passive particle movement*

Figure 6 summarizes the general patterns of particle redistribution in the passive particle release experiments. The two panels display the three-year average (2007–2009) for particles released on 1 May (left) and 29 August (right) and subsequently tracked for 60 days. We choose these release dates to represent early- and late-season dates when infective elements might be released during the infection period (~June through early October) for *H. nelsoni* in Delaware Bay (Ford and Haskin, 1982). Three-year mean passive particle trajectories may be summarized as follows.

Particles released in the lower bay (at site 1 on the New Jersey side, and site 2 on the Delaware side) are retained to a far greater extent than particles released from more upper-bay sites. For example, of the particles released from site 1 in the Leased Grounds 46% (May) and 43% (September) remain in the surrounding region B after 60 days. The retention percentages for site 2 are comparable: 55% (May) and 36% (September). The relatively high retention rates in the lower bay are explained by the circulation patterns that develop as the bay widens. As the width increases in the lower bay, the strongest along-bay flows are found to be confined to approximately the middle third of the cross-bay width. Regions of weak

8. We do not know if MSX is passive or neutrally buoyant because the infective stage or any free living stages have not been identified. It is plausible that other factors may account for its movement such as buoyancy or perhaps an intermediate host that can migrate to some degree.

9. Passive particles are both transported by the simulated three-dimensional velocity field, and mixed vertically by a random walk process whose amplitude is obtained from the ROMS turbulent closure sub-model. The passive particles have no active behavior.

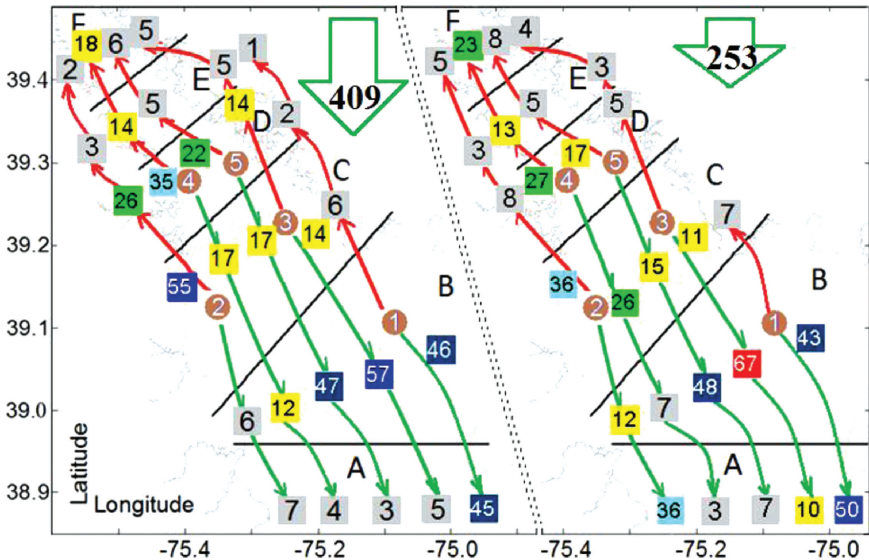


Figure 6. Particle transport and retention percent on the 60th tracking day since release dates 1 May (left) and 29 August (right). The numbers in the squares show the percent of particles released at each of the sites 1–5 that reach each of the 6 sub-regions A–F after 60 days. Arrows with numbers are the 60-day-average river discharge rates ( $\text{m}^3/\text{s}$ ) over the same period. Each panel is a three-year average over the years 2007, 2008 and 2009. The colored squares are used to highlight the larger numbers with an interval of 10%: grey 0–10, yellow 11–20, green 21–30, light blue 31–40, dark blue 41–50, blue 51–60, and red 61–70%, respectively.

flow develop on either flank, increasing the residence times of particles released at these locations. The increased residence times of passive particles in region B is consistent with the hypothesis, based on elevated MSXP in Leased Ground oysters, that *H. nelsoni* infective elements are concentrated in the lower bay and become diluted in an upbay direction (Ford and Haskin, 1982).

The effectiveness of upbay particle transport varies considerably with the location of particle release. Direct communication of particles from the lower bay to the upper bay (e.g., from release site 1 to regions C through F) is inefficient. Rather, delivery of passive particles to the upper-bay (regions E and F) is primarily from the Delaware side of the bay at release location 4, with a lesser contribution from release sites 2, 3 and 5. The fact that sites 2 and 5 are closest neighbors to site 4 suggests that passive particles from 2 and 5 that successfully reach upbay locations may do so by first passing through the Delaware side of region D near release site 4. This is clearly the efficient upbay path for particles released at site 2, immediately downbay of site 4. But do particles released at site 5 reach upbay regions via the New Jersey or the Delaware side of the bay? This will depend on the net transverse circulation.

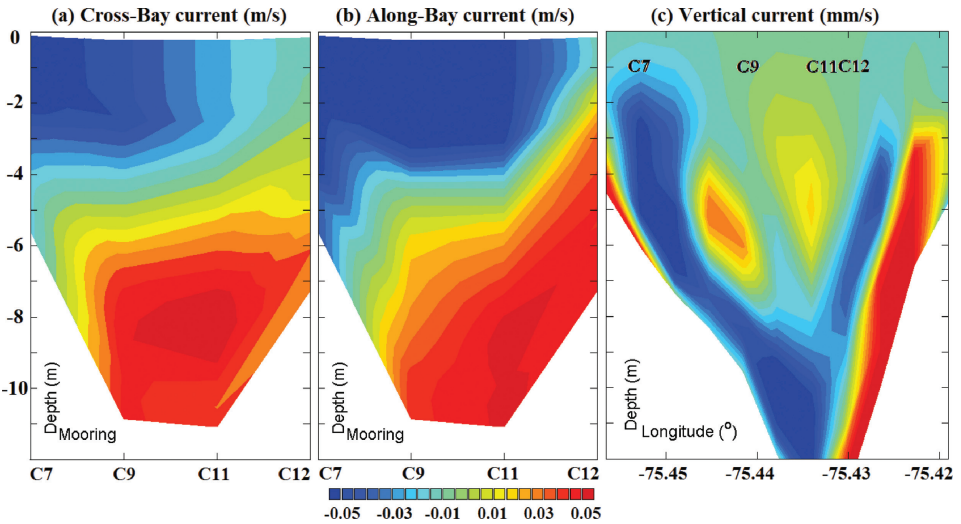


Figure 7. Cross-bay sections of time-averaged currents for July 2011: (a) observed (DBMDP) cross-bay component of vector current (m/s), (b) observed (DBMDP) along-bay component of vector current (m/s), and (c) simulated vertical current (mm/s). The mooring locations C7–C12 are indicated in Figure 1c. Positive values of the color-bar correspond to transport from Delaware towards New Jersey [in (a)], upbay transport (b), and upwards transport (c).

Figure 7 shows the time-mean circulation July 2011 in the cross-bay plane at the location of the DBMDP moorings (Fig. 1c). The time-mean circulation in the plane of the mooring array is determined to be in the counter-clockwise sense. This residual circulation is consistent with the primary route for simulated passive transport to the upper bay. Particles released on the Delaware side of the bay are preferentially transported across and down into the shipping channel, where transport upbay is enhanced. It also suggests that particles from both sites 2 and 5 reach upbay locations, at least in part, via site 4.

Figure 8 shows the monthly cross-bay particle exchange between sites 4 and 5 in region D, showing the percent of particles released at site 5 that successfully transit to the New Jersey side of the bay, as well as those released at site 4 that arrive on the New Jersey side. There are approximately net 8~15% particles successfully transported from NJ side (site 5) to Delaware side (site 4).

Powell *et al.* (this issue) report on the spatial distribution of seston food resources for oysters in Delaware Bay in 2009–2010. These analyses reveal that bay locations fall into two primary groups, one covering the bulk of the sites on the New Jersey side of the bay where seston values tend to fall below the bay-wide average and the other covering the sites on the Delaware side of the bay where seston values are routinely higher. However, sites associated with the uppermost New Jersey oyster beds [Arnolds and upbay; Powell *et al.* (this issue, Fig. 1)] are consistently more similar to sites down-estuary on the Delaware side of the bay than down-estuary on the New Jersey side. This similarity is consistent with the

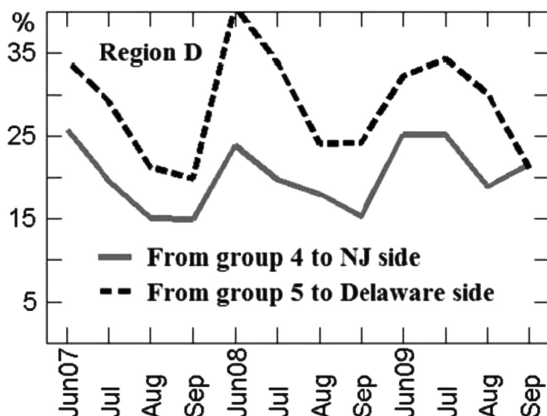


Figure 8. Monthly cross-bay particle exchange in region D. The solid (dashed) line shows the percent of particles released at site number 4 (5) that successfully transit to the NJ (DE) side of the shipping channel.

finding here of the tendency for passive particles released on the Delaware side of the bay to preferentially reach upbay regions.

Lastly, it may be noted from Figure 6 that the patterns and percentages of passive transfer display a substantial degree of spring-to-fall variation. For example, the net transport of particles to upper-bay regions is enhanced by approximately 30% in fall (September) relative to spring (May). This is qualitatively consistent with the normal seasonal variation in river inflow, which is characterized by enhanced input in the spring. Interestingly, export of passive particles from the Delaware side (site 2) to the open ocean is significantly greater in fall than in spring despite the seasonal patterns in river discharge.

#### *b. Inter-annual variability in particle redistribution*

The type of information shown in geographical perspective in Figure 6 can be compactly summarized in the form of a location probability matrix (LPM). In the LPM, the probability that particles released at each of the five sites (1 through 5) will terminate in one of the six Delaware Bay sub-domains (A through F) is tabulated in a 5-by-6 matrix. Figure 9 shows a suite of LPMs for particle releases on May 1 and August 29 for each of the years 2007, 2008 and 2009.

As noted above, the primary route for passive particles to reach upbay regions is via release site 4. However, a strong temporal dependence in the effectiveness of this transfer pathway is indicated. If we use as a metric of net transfer effectiveness from site 4 the combined percent of arrivals at regions E and F on days 30 and 60, then the periods of the most successful upbay transfer are Fall 2007, Spring 2008 and Fall 2009. Spring 2008 is also anomalous in other respects. Note in particular that it displays the most significant direct upbay transfer from release area 1 of any of the other years and seasons.

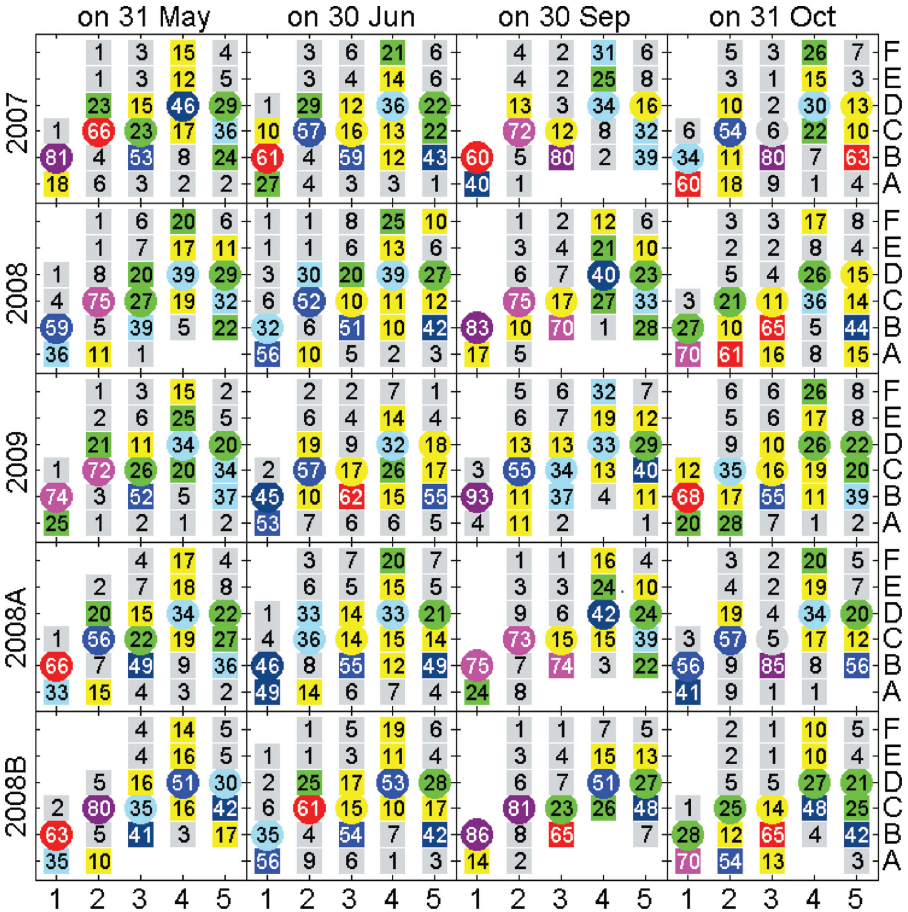


Figure 9. Percent of particles released at each of the sites 1–5 (x-axis) that terminate in each of the 6 sub-regions A–F (y-axis) after 30 (columns 1 and 3) or 60 days (columns 2 and 4). The years labeled 2008A and 2008B are the no-wind and increased bottom stress cases, respectively. Particles were released on 1 May, 1 May, 29 August and 29 August for the columns labeled 31 May, 30 June, 30 September and 31 October, respectively. Circled numbers correspond to the regions within which the particles of the respective groups were released, i.e., to retention percentages. The colored squares and circles are used to highlight the larger numbers with an interval of 10%: grey 0–10, yellow 11–20, green 21–30, light blue 31–40, dark blue 41–50, blue 51–60, red 61–70%, pink 71–80, and purple 81–90%, respectively.

The sensitivity experiments 2008A and 2008B are both instructive. With the wind forcing removed (2008A), the anomalous direct communication from release site 1 to the upper-bay in May/June 2008 is lost (Fig. 9). Although not the dominant mechanism for particle redistribution, the wind was apparently consequential in enhancing upbay transport in May/June 2008. As discussed above, the mean spring winds are directed cross-bay from the southwest, and were particularly strong in 2008. Although other dynamical explanations are possible,

the enhanced upbay communication of particles in spring 2008 is consistent with upbay geostrophic flow arising from an enhanced wind-induced cross-bay pressure gradient (i.e. sea surface tilt).

Small reductions in upbay transport of passive particles from release site 4 accompany both the removal of wind forcing and an increase in the bottom stress coefficient (Fig. 9; experiments 2008A and 2008B respectively). Nonetheless, transport via site 4 remains the primary transport route. The decrease in upbay particle transport with increased bottom drag is consistent with the reduced amplitude of the tidal circulation that results from the enhanced bottom stress (section 2.d.iv).

Finally, we note that summer 2008 is also a period of strong cross-bay particle exchange in region D with approximately net 15% particles successfully transported from NJ side (site 5) to Delaware side (site 4) in June 2008 (Fig. 8). In other months of 2007–09, the net percent is below 10%. The anomalous period of high upbay MSXP in Fall 2008 therefore does correspond to a year in which both cross-bay and upbay transport of passive particles was enhanced in May and June.

## 5. Summary and discussion

We have developed a high-resolution hydro-dynamical model for the Delaware Bay forced by hydrological inputs from six rivers and atmospheric inputs of momentum, heat and moisture. Model validation against intensive *in situ* datasets in the years 2000 and 2010–2011 shows the model to possess significant skill in predicting variations in water level, temperature, salinity and currents. Both seasonal and tidal-frequency signals are accurately reproduced with little bias.

The resulting Delaware Bay model has been applied to quantify the relationship between observed *Haplosporidium nelsoni* infection prevalence (MSXP) and concurrent physical conditions in the bay. To do so, simulations of circulation and environmental conditions in Delaware Bay were performed for five multi-year periods that displayed different combinations of MSXP and environmental conditions, and that covered a total of sixteen years. Subsequent statistical analysis and passive particle releases were used to explore the connections between MSXP and (e.g.) salinity and temperature. The hypothesis under-lying these analyses has been that elevated levels of MSXP at low-salinity, upbay locations depend upon a source of infective stages, an effective means of upbay transport, and environmental conditions hospitable to the parasite. We further hypothesized that the source of infection comes from lower-bay regions where infection prevalence (until the onset of resistance in the oyster population in the late 1980s) was relatively high and that the abundance of infective stages in any given year was proportional to that prevalence. In subsequent years, molecular assays have demonstrated that *H. nelsoni* remains pervasive in the bay and continues to show an upbay to downbay increase in prevalence (Ford *et al.*, this issue).

Results from the correlation analysis suggest that MSXP may be related to multiple physical factors, depending on location and time of year. As has been hypothesized (but not quantified) previously, MSXP is significantly correlated with river flow and salinity, especially at upbay locations. In addition, at mid-bay locations the combined influence of temperature and salinity – via the salty-warm water area index – is particularly well correlated with observed levels of MSXP.

We can examine our three-part hypothesis (i.e., that MSPX in the upper bay depends on availability of infective element, an effective upbay transport mechanism and favorable temperature and salinity conditions) by inspecting disease and water properties in 2007–2009 when we have data on the prevalence of *H. nelsoni* in the upper and lower bay regions from both molecular (PCR) and histological assays (see Ford *et al.*, Figs. 1 and 4, this issue for prevalence details) as well as particle transport simulations. In 2007, the relative abundance of *H. nelsoni* at two lower-bay sites where the parasite has always been present (New Beds and Cape Shore) was moderately high. Transport potential to Region E was strong and prevalence in that region, represented by Arnolds Bed, was also moderately high.

More instructive is a comparison between 2008 and 2009. In 2008, downbay prevalence was very high, upbay transport potential was strong to upbay Regions E and F, and *H. nelsoni* prevalence spiked in both regions. In contrast, *H. nelsoni* was not detected in either upbay region in 2009, despite moderate upbay transport potential that year (Fig. 9). As judged by the near absence of infections at the Cape Shore site during the summer and fall of 2009 and in September and November at New Beds, we conclude that infective stages were relatively scarce in the lower-bay in 2009, which would have limited their availability for upbay transport even though the mechanism existed. In addition, salinity on the upper-bay sites was considerably lower in 2009 than in 2008 so that the environment was less conducive to *H. nelsoni* survival and its ability to infect and proliferate in oysters.

Although the above comparison appears to be consistent with a scenario in which “free” infective stages are moved upbay from a lower-bay source, we urge caution in coming to such a conclusion. For instance, another host, such as a weakly swimming zooplankter, could equally well be transported upbay in the same manner and infective stages could be released “on site.” Alternatively, there may not be a single source region, but sources throughout the bay that respond similarly to factors that influence the abundance of infective particles in all areas at the same time. In this regard, it is important to note that Figures 6 and 9 show relative potential transport from release locations rather than absolute values. The absolute transport potential will depend upon the abundance of particles released at a particular location.

Another unknown factor complicating the understanding of *H. nelsoni* transmission within the bay is the life-span of whatever stage is transported. The parasite develops a spore, which appears to be designed for distance transmission and the ability to survive for extended periods outside a host. It has a thick wall (Rosenfield *et al.*, 1969) and filamentous appendages (Burreson and Reece, 2006), which should protect it and minimize

sinking, respectively, during transport. In addition, we have found evidence of spore stages throughout Delaware Bay (Barber and Ford, 1992) and have kept spores refrigerated in seawater for months without visible damage to the sporoplasm and nucleus inside (Ford, unpublished).

Lastly, future changes to the thermal and hydrologic conditions may be expected to have a profound influence on MSXP in Delaware Bay. A warming climate is expected to be accompanied by changes in both precipitation patterns and ice and snow cover (Rudolf *et al.*, 1994; Lemke *et al.*, 2007). All of these effects will mutually combine to establish future levels and distributions of MSXP. A natural next step is to inquire into the potential impacts of future climate variability on circulation, tracer fields, and MSXP in Delaware Bay using the modeling tools developed here. A sequence of climate sensitivity studies addressing these issues is underway.

*Acknowledgments.* This study has been supported by the National Science Foundation Ecology of Infectious Diseases program (OCE06-22672). Funding was also provided by the Army Corps of Engineers under their Section 22 funding authority, contract #W912BU-11-C-0004, through the Seaboard Fisheries Institute, in collaboration with the sponsor, the South Jersey Port Corporation, a public agency of the State of New Jersey. Finally, the first author received Fellowship support from the DuPont Corporation and the New Jersey agriculture experiment station. Dr. Robert Chant (Rutgers University) provided DBMDP salinity, temperature, and current in 2010–2011. Dr. David Robinson (Rutgers University), Dr. Kevin Brinson (University of Delaware), and Dr. Daniel Leathers (University of Delaware) provided the DEOS solar radiation data. Dr. Kenneth Brink provided software and patiently helped correct our manuscript for which we are very grateful. We thank the three anonymous reviewers for their thoughtful comments that have led to significant improvement in the presentation and interpretation of these results.

## APPENDIX

### Quantitative model validation

The Delaware Bay hydrodynamic model has been validated against a number of independent data sets (described in Section 2d). Quantitative evaluation of model simulations for the years 2000 and 2010–2011 has been performed using several metrics, including the Taylor diagram (Taylor, 2001), the system bias, and the skill score utilized by Warner *et al.* (2005). The latter varies from zero (no skill) to 100% (perfect agreement) and is given by the formula:

$$WSK = \left\{ 1 - \frac{\sum_{n=1}^{N_s} |X_{\text{mod}}(n) - X_{\text{obs}}(n)|^2}{\sum_{n=1}^{N_s} [ |X_{\text{mod}}(n) - X_{\text{obsm}}| + |X_{\text{obs}}(n) - X_{\text{obsm}}| ]^2} \right\} \times 100\%$$

where  $X_{\text{mod}}$  and  $X_{\text{obs}}$  are the simulated and observed time series,  $X_{\text{modm}}$  and  $X_{\text{obsm}}$  are the respective temporal means, and  $N_s$  is the number of samples.

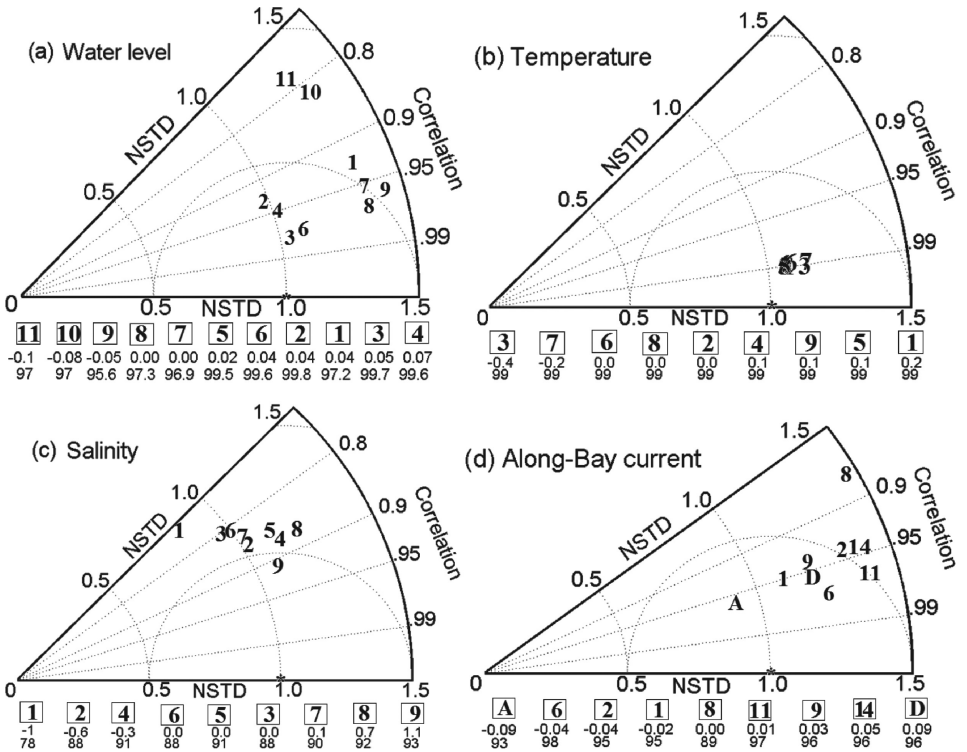


Figure A.1. Taylor diagrams (Taylor, 2001) showing model-data comparisons for: (a) water level (m) at the 11 stations shown in Figure 1a, computed from hourly data from 11 Jun to 31 Dec 2000; (b) and (c) temperature (°C) and salinity observed and simulated at stations 1–9 shown in Figure 1b, based on 4416 hourly data from 13 May to 12 November 2000; (d) vertically averaged along-bay current at nine moorings (A, D, C1–2, C6, C8–9, C11 and C14; Fig. 1c) with sample sizes 1808–6903 from July 2010 to September 2011. The two rows of numbers below each Taylor diagram are the bias (mean of observations minus mean of simulation; upper row of numbers) and the skill score (lower row of numbers).

All of these metrics may be summarized on a single modified Taylor diagram. Figure A1 shows the resulting diagrams for water level, temperature and salinity observed in the year 2000, and for along-bay currents measured in the years 2010–2011. There are several statistical quantities summarized in the resulting Taylor diagrams: (1) the correlation coefficient (correlation) between data and simulation indicated on the azimuthal axis; (2) the standard deviation normalized to data (NSTD) expressed by the radial distance from the origin to the “test” points; and (3) the centered-pattern RMS difference (the square root of the mean square difference between the observed and simulated de-measured time series) given by the distance from the pink star to a “test” point. Finally, (4) the system bias (mean of data minus mean of the simulation) is shown in the first row of numbers below the Taylor diagram; and

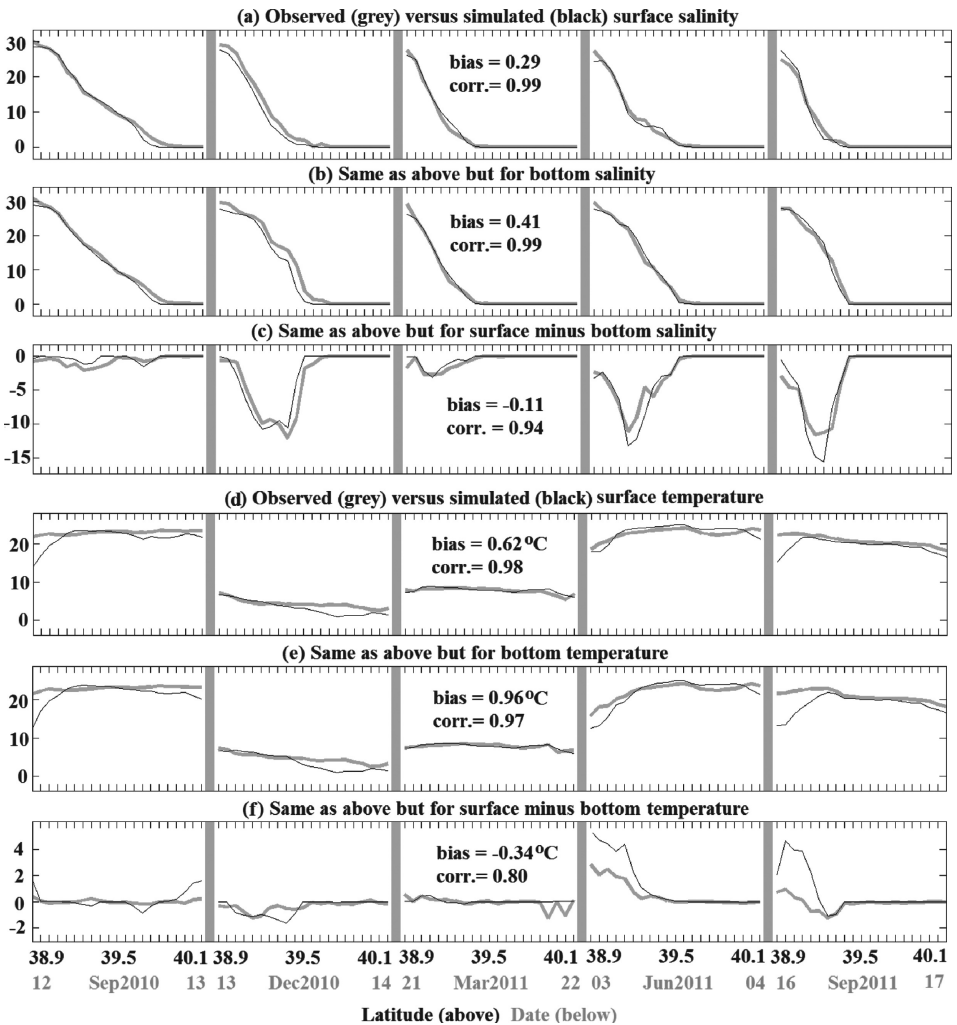


Figure A.2. Observed (grey line) versus simulated (black line): (a, b, c) surface and bottom salinity, and their difference; and (d, e, f) surface and bottom temperature, and their difference. The data cover five seasons from September 2010 to September 2011 from left to right frames and span from low (38.9°N) to up (40.1°N) Bay. In each season, there is one survey lasting a few days (indicated on the last line of this Figure) to observe once on each of the twenty-one locations (latitude range is given on the last but one line of this Figure). There are 105 salinity and temperature samples for the five surveys on the twenty-one locations. These 105 salinity samples are concatenated to form one “time-space” series for statistical analysis.

5) the skill score (%) is shown by the numbers on the second line. For a perfect simulation, correlation = 1, NSTD = 1, centered-pattern RMS difference = 0, bias = 0 and skill = 100%. A summary of the primary results from these statistical time-series comparisons has been given in Section 2d.

The statistical measures shown in Figure A1 refer to temporal variability at single spatial points. Another important measure of model fidelity pertains to the spatial distribution of properties in both the horizontal and the vertical. The vertical gradients in temperature and salinity (*i.e.*, the stratification) are of obvious dynamical interest. Fortunately, the along-bay surveys of T and S made in 2010–2011 provide an opportunity to assess how well the model simulations recover the along-bay variations in salinity and temperature as well as the resulting vertical stratification.

As shown in Figure A2, the simulations recover the top-to-bottom salinity difference with great skill. Both the along-bay location of the salt wedge and its strength are recovered. Temperature stratification is also recovered with some skill; however, the model is shown to be too cold in the summer months at the mouth of the bay. We conclude from this that the model omits (or misrepresents) some aspect of the heat budget as we progress downbay and out onto the shelf. Candidate explanations include the absence of heat input through the open cross-shelf boundaries and/or a poorly chosen parameter in the heat budget. One possibility for the latter is the water type. The single value applied everywhere in these simulations has been chosen to be appropriate for the Bay proper and may be less well suited to the water column in the lower Bay. In particular, note from our sensitivity studies that the use of water type 7 reduces the temperature of the water column. That the model is too cold in the lower bay is therefore at least consistent with the hypothesis that water type 7 becomes a decreasingly appropriate choice as we move downbay and out onto the shelf.

#### REFERENCES

- Andrews, J. D. 1964. Oyster mortality studies in Virginia. IV. MSX in James River public seed beds. *Proc. Nat. Shellfish. Assoc.*, 53, 65–84.
- 1966. Oyster mortality studies in Virginia V. Epizootiology of MSX, a protistan pathogen of oysters. *Ecology*, 47, 19–31.
- 1983. *Minchinia nelsoni* (MSX) infections in the James River seed-oyster area and their expulsion in spring. *Estuar. Coast. Shelf Sci.*, 16, 255–269.
- Barber, R. D., S. A. Kanaley and S. E. Ford. 1991. Evidence for regular sporulation by *Haplosporidium nelsoni* (MSX) (Ascetospora: Haplosporidiidae) in spat of the American oyster, *Crassostrea virginica*. *J. Protozool.*, 38, 305–306.
- Barber, R. D. and S. E. Ford. 1992. Occurrence and significance of ingested haplosporidan spores in the eastern oyster, *Crassostrea virginica* (Gmelin, 1791). *J. Shellfish Res.*, 11, 371–375.
- Burreson, E. M. and K. S. Reece. 2006. Spore ornamentation of *Haplosporidium nelsoni* and *Haplosporidium costale* (Haplosporidia), and incongruence of molecular phylogeny and spore ornamentation in the haplosporidia. *J. Parasitology*, 92, 1295–1301.
- Cahill, B., O. Schofield, R. Chant, J. Wilkin, E. Hunter, S. Glenn and P. Bissett. 2008. Dynamics of turbid buoyant plumes and the feedbacks on near-shore biogeochemistry and physics. *Geophys. Res. Lett.*, 35, L10605, doi:10.1029/2008GL033595.

- Chelton, D. B. 1983. Effects of sampling errors in statistical estimation. *Deep-Sea Res.*, *30*, 1083–1101.
- Emery, W. J. and R. E. Thomson. 2004. *Data Analysis Methods in Physical Oceanography*, Elsevier, 638 pp.
- Ford, S. E. 1985. Effects of salinity on survival of the MSX parasite *Haplosporidium nelsoni* (Haskin, Stauber, and Mackin) in oysters. *J. Shellfish Res.*, *5*, 85–90.
- Ford, S. E., B. Allam and Z. Xu. 2009. Using bivalves as particle collectors and PCR detection to investigate the environmental distribution of *Haplosporidium nelsoni*. *Dis. Aquatic Org.*, *83*, 159–168.
- Ford, S. E and D. Bushek. 2012. Development of resistance to an introduced marine pathogen by a native host. *J. Mar. Res.*, *70*, 205–223.
- Ford, S. E. and H. H. Haskin. 1982. History and epizootiology of *Haplosporidium nelsoni* (MSX), an oyster pathogen, in Delaware Bay, 1957–1980. *J. Invertebr. Pathol.*, *40*, 118–141.
- Ford, S., E. Powell, J. Klinck and E. Hofmann. 1999. Modeling the MSX parasite in eastern oyster (*Crassostrea virginica*) populations. I. Model development, implementation, and verification. *J. Shellfish Res.*, *18*, 475–500.
- Ford, S. E., E. Scarpa and D. Bushek. 2012. Spatial and temporal variability in disease refuges in an estuary: implications for the development of resistance. *J. Mar. Res.*, *70*, 253–277.
- Ford, S. E. and M. R. Tripp. 1996. Disease and defense mechanisms, in *The Eastern Oyster: Crassostrea virginica*, V. S. Kennedy, R. I. E. Newell and A. F. Eble, eds., Maryland Sea
- Haskin, H. H. and J. D. Andrews. 1988. Uncertainties and speculations about the life cycle of the eastern oyster pathogen *Haplosporidium nelsoni* (MSX), in *Disease Processes in Marine Bivalve Molluscs*, W. S. Fisher, ed., American Fisheries Society, 5–22.
- Haskin, H. H. and S. E. Ford. 1982. *Haplosporidium nelsoni* (MSX) on Delaware Bay seed oyster beds: a host-parasite relationship along a salinity gradient. *J. Invertebr. Pathol.*, *40*, 388–405.
- Lemke, P., J. Pen, R. B. Alley, I. Allison, J. Carrasco, G. Flato, Y. Fujii, G. Kaser, P. Mote, R. H. Thomas and T. Zhang. 2007. Observations: Changes in Snow, Ice and Frozen Ground, in *Climate Change (2007)*, The Physical Science Basis. Contribution of Working Group I to the Fourth Assessment Report of the Intergovernmental Panel on Climate Change, S. Solomon, D. Qin, M. Manning, Z. Chen, M. Marquis, K. B. Averyt, M. Tignor and H. L. Miller, eds., Cambridge University Press, 996 pp.
- Liu, Y., P. MacCready, B. M. Hickey, E. P. Dever, P. M. Kosro and N. S. Banas. 2009. Evaluation of a coastal ocean circulation model for the Columbia River plume in summer 2004. *J. Geophys. Res.*, *114*, C00B04, doi:10.1029/2008JC004929.
- Marchesiello, P., J. C. McWilliams and A. Shepovkin. 2001. Open boundary conditions for long-term integration of regional ocean models. *Ocean Model.*, *3*, 1–20.
- Mellor, G. L. and T. Yamada. 1982. Development of a turbulent closure model for geophysical fluid problems. *Reviews of Geophysics and Space Physics*, *20*, 851–875.
- Mesinger, F., G. DiMego, E. Kalnay, K. Mitchell, P. C. Shafran, W. Ebisuzaki, D. Jovi, J. Woollen, E. Rogers, E. H. Berbery, M. B. Ek, Y. Fan, R. Grumbine, W. Higgins, H. Li, Y. Lin, G. Manikin, D. Parrish, and W. Shi. 2006. North American regional reanalysis. *Bull. of Amer. Meteor. Society*, *87*, 343–360.
- Mukai, A. Y., J. J. Westerink, R. A. Luettich and D. Mark. 2002. East coast 2001, a tidal constituent database for the western North Atlantic, Gulf of Mexico and Caribbean Sea, Tech. Rep. ERDC/CHL TR-02-24, 196 pp.
- Narváez, D. A., J. M. Klinck, E. N. Powell, E. E. Hofmann, J. Wilkin and D. B. Haidvogel. 2012a. Modeling the dispersal of eastern oyster (*Crassostrea virginica*) larvae in Delaware Bay. *J. Mar. Res.*, *70*, 381–409.

- 2012b. Circulation and behavior controls on dispersal of eastern oyster (*Crassostrea virginica*) larvae in Delaware Bay. *J. Mar. Res.*, *70*, 411–440.
- Paraso, M. C., S. E. Ford, E. N. Powell, E. E. Hofmann and J. M. Klinck. 1999. Modeling the MSX parasite in eastern oyster (*Crassostrea virginica*) populations. II. Salinity effects. *J. Shellfish Res.*, *18*, 501–516.
- Paulson, C. A. and J. J. Simpson. 1977. Irradiance measurements in the upper ocean. *J. Phys. Oceanogr.*, *7*, 952–956.
- Powell, E. N., K. A. Ashton-Alcox, J.N. Kraeuter, S.E. Ford and D. Bushek. 2008. Long-term trends in oyster population dynamics in Delaware Bay: Regime shifts and response to disease. *J. Shellfish Res.*, *27*, 729–755.
- Powell, E. N., D. E. Kreeger, J. M. Morson, D. B. Haidvogel, Z. Wang, R. Thomas and J. E. Gius. 2012. Oyster food supply in Delaware Bay: Estimation from a hydrodynamic model and interaction with the oyster population. *J. Mar. Res.*, *70*, ???–???
- Rosenfield, A., L. Buchanan and G. B. Chapman. 1969. Comparison of the fine structure of spores of three species of *Minchinia* (Haplosporida, Haplosporidiidae). *J. Parasitology*, *55*, 921–941.
- Rudolf, B., H. Hauschild, W. Rueth and U. Schneider. 1994. Terrestrial precipitation analysis: Operational method and required density of point measurements, in *Global Precipitations and Climate Change*, M. Buboïs and F. Désalmand, eds., NATO ASI Series I, *26*, Springer Verlag, Berlin, 173–186.
- Shchepetkin, A. F. and J. C. McWilliams. 2005. The regional ocean modeling system: A split-explicit, free-surface, topography-following coordinate oceanic model. *Ocean Model.*, *9*, 347–404.
- Smolarkiewicz, P. K. and W. W. Grabowski. 1990. The multidimensional positive definite advection transport algorithm: nonoscillatory option. *J. Comput. Phys.*, *86*, 355–375.
- Taylor, K. E. 2001. Summarizing multiple aspects of model performance in a single diagram. *J. Geophys. Res.*, *110*, C11021, doi:10.1029/2005JC002902.
- Umlauf, L. and H. Burchard. 2003. A generic length-scale equation for geophysical turbulence models. *J. Mar. Res.*, *61*, 235–265.
- Warner, J. C., W. R. Geyer and J. A. Lerczak. 2005. Numerical modeling of an estuary: A comprehensive skill assessment. *J. Geophys. Res.*, *110*, C05001, doi:10.1029/2004JC002691.
- Zhang, W., J. Wilkin and R. Chant. 2009. Modeling the pathways and mean dynamics of river plume dispersal in New York Bight. *J. Phys. Oceanogr.*, *39*, 1167–1183.

Received: 24 October, 2011; revised: 25 July, 2012.